

# Electrostatically driven magnetic field micromodulator with continuous modulating angle and large shifting range

Kun Liu<sup>1,2</sup>, Huaiqiang Yu<sup>1</sup>, Yitong Cao<sup>1</sup>, Zhihong Li<sup>1</sup>

<sup>1</sup>National Key Laboratory of Science and Technology on Micro/Nano Fabrication, Institute of Microelectronics, Peking University, Beijing, People's Republic of China

<sup>2</sup>School of Computer and Information Engineering, Peking University Shenzhen Graduate School, Shenzhen, People's Republic of China  
E-mail: zhhli@pku.edu.cn

Published in Micro & Nano Letters; Received on 15th May 2013; Accepted on 24th June 2013

Presented is a novel magnetic field modulator made up of permanent magnets, and having a torsional electrostatically driven structure, which was fabricated by electrodeposition and released by KOH solution wet etching. The magnetic properties of the electrodeposited CoNiMnP micromagnets and the torsional angle with respect to the driving voltage of the microdevice have been measured, and the modulation of the magnetic field has been demonstrated. The low power consumption micromodulator, which can achieve a continuous torsional angle of 0°–18° and a pull-in angle of 54.7°, has its own advantage over the traditional magnetic field modulating devices. The novel modulator has not only provided a more effective approach for magnetic field modulation, but also offered a torsional carrier actuator to be integrated with various functional materials or components in many applications.

**1. Introduction:** In recent years, magnetic microelectromechanical systems (MagMEMS) [1, 2] have received a lot of attention owing to their additional functionality in electrical microsystems. The integration of magnetic components will expand the application of microelectromechanical systems [3]. Compared with electromagnetic components like microcoils and microinductors, permanent magnetic components exhibit a big advantage in efficiency and power consumption when they generate the same magnitude of magnetic field [1, 4]. Although a lot of permanent or hard micromagnets have been widely used in microscale applications like micromotors and energy harvesters [5], seldom have they been employed as a critical component of microsystems for spatial magnetic field modulation.

In this Letter, we present a novel electrostatically driven magnetic field modulator with the integration of electroplated permanent magnets. The motion of micromagnets can change the surrounding magnetic field, without the requirement of exciting electric current. Owing to electrostatically driven mode and permanent magnets integration, the micromodulator achieves zero static power consumption, which meets the requirement of remotely controlled microsystems loaded on flying migratory birds like a homing pigeon (*Columbia livia*), whose fly orientation can be disturbed or roughly controlled by an externally induced magnetic field [6–9]. Unlike the traditional magnetic field exciting components [10–12] formerly employed by avian behaviour researchers, the novel microactuator [13] we have utilised can achieve a continuous modulating angle and a large shifting range, which will make the smart system an excellent equipment for research of avian artificial navigation.

**2. Working principle and device design:** From the variety of prototypes provided by well developed microoptoelectromechanical system (MOEMS) devices, such as torsional optical switches [14, 15] and optical scanning mirrors [16–18], an electrostatically driven torsional plate was chosen as the carrier actuator to be combined with permanent magnetic components. The schematic view and lateral dimension parameters of the proposed microactuator are shown in Fig. 1. Although applying a certain voltage between the two electrodes of the microactuator, the micropermanent magnets will rotate over the same angle with

the carrier plate, causing the change of the surrounding magnetic field both in amplitude and in direction.

Degani *et al.* [19] and Zhang *et al.* [20] have analysed the pull-in effect and the static characteristics of the electrostatic torsional micromirror. Since it is not necessary to consider the high frequency response of the microactuator in magnetic field modulation, only the static or quasi-static characteristics of the present device have to be analysed.

In static state condition, the two torques applied on the torsional beam, the electrostatic torque and the mechanical restoring torque, must be balanced. The electrostatic torque  $T_e$ , generated by the driving voltage, can be described as

$$T_e = \frac{\varepsilon}{2} \frac{W_m V^2}{(\theta_{\text{Full\_Swing}} - \theta)^2} \ln \frac{L_m}{L_0} \quad (1)$$

where  $\varepsilon$  is the permittivity of the dielectric layer, here in our case, the dielectric layer is air and the permittivity approximately equals to vacuum permittivity  $\varepsilon_0$ .  $W_m$  and  $L_m$  are the width and length of the mirror part.  $\theta$  and  $\theta_{\text{Full\_Swing}}$  are the torsional angle and full swing torsional angle (here it is 54.7° according to KOH anisotropic etching characteristic).  $L_0$  is the distance from the mirror to the KOH mask edge and  $V$  is the applied driving voltage.

Equation (1) indicates that a larger area of the mirror plate will be helpful to increase the electrostatic torque, which is the same as that in the case of electrostatic force in parallel capacitor actuators. Meanwhile, the mirror plate area cannot increase without limitation because of the fabrication capability, and an actuator with too large size will drop off from the substrate in the wet etching process.

The other torque, the mechanical restoring torque, is generated by shear stress of the torsional beam. It is also proportional to the torsional angle  $M_r = K_\theta \theta$ , and can be described as

$$M_r = K_\theta \theta = \frac{Et^3 w}{(1 + \nu)l} \left[ \frac{1}{3} - 0.21 \frac{t}{w} \left( 1 - \frac{t^4}{12w^4} \right) \right] \theta \quad (2)$$

where  $K_\theta$  and  $\theta$  are the torsional stiffness and torsional angle of the torsional beam,  $l$ ,  $w$  and  $t$  are the length, width and thickness of the

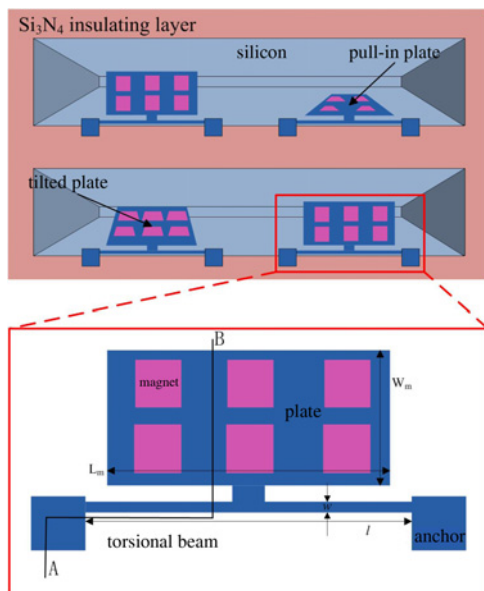


**Figure 1** Schematic view of microactuators array and zoom in view of single device

beam, respectively,  $E$  and  $\nu$  are the Young's modulus and the Poisson ratio of torsional beam.

It is shown in (2) that the most important factor to the mechanical restoring torque is the thickness of the torsional beam, the cubic of which is proportional to the torsional stiffness. A smaller beam-width will also result in a lower torsional stiffness. Meanwhile, the dimensions of the torsional beam are also limited by the feature size and the uniformity of the fabrication process.

Modal analysis by ANSYS<sup>TM</sup> shows that the resonant frequency of the first vibration mode lies far from that of high-order vibration modes, so only the torsional motion of the microactuator needs to be considered. By equalising (1) and (2) we can obtain a relationship between the torsional angle and applied voltage, which indicates that a larger area of the mirror plate, and a lower width or thickness of the torsional beam will produce a lower driving voltage and pull-in voltage, but they are also limited by the ability and yield of the fabrication process. Therefore the width and thickness of the torsional beam are decided to be minimised under current fabrication process limits, which are both equal to  $2.3 \mu\text{m}$  after electroplating. Other dimensions can be varied in different conditions, here in this case, we choose  $760 \mu\text{m}$  for the length of the torsional beam, and  $600$  and  $360 \mu\text{m}$  for the length and width of the mirror plate, respectively.

**3. Fabrication, characterisation and experimental setup:** To realise the large shifting range of magnetic field modulation, a large portion of silicon must be removed from the substrate in the fabrication and bulk micromachining process is acquired. The fabrication process flow of our magnetic field micromodulator is illustrated in Fig. 2, which was a hybrid integration of the surface sacrificial process and the bulk micromachining process.

The process started with a thermal oxidation of  $3000 \text{ \AA}$   $\text{SiO}_2$  on a 4-inch (100) silicon wafer, and a layer of  $1000 \text{ \AA}$   $\text{Si}_3\text{N}_4$  was deposited by low-pressure chemical vapour deposition (LPCVD) on  $\text{SiO}_2$ . After lithography patterning, both layers were etched by reactive-ion etching (RIE) as the KOH etching mask. Then, a layer of  $4000 \text{ \AA}$  Al was evaporated on a  $\text{Si}_3\text{N}_4$  layer and patterned by wet etching as a sacrificial layer for final KOH etching. In the following step, an adhesion layer of  $150 \text{ \AA}$  Cr and a seed layer of  $2000 \text{ \AA}$  Cu for electroplating were sputtered, then a  $2.3 \mu\text{m}$  Ni structure layer was electroplated to form the torsional beam, mirror and anchor part of the microactuator. Following the

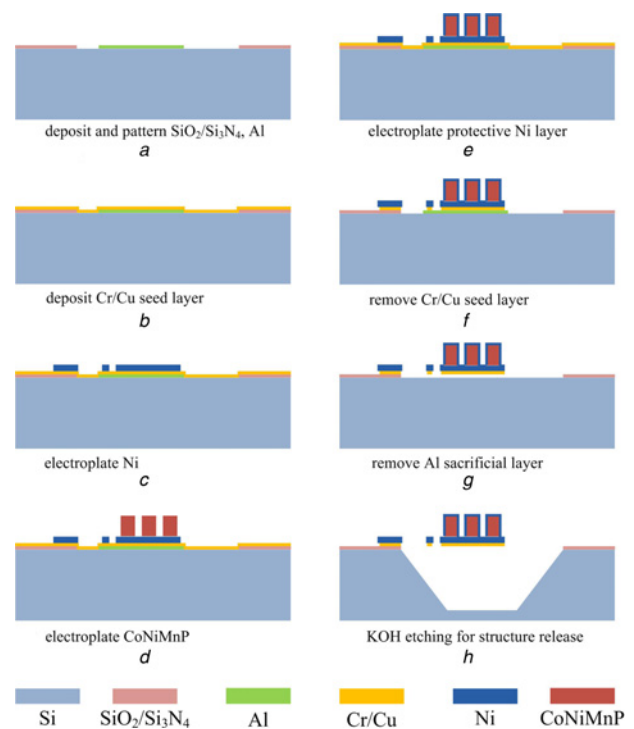


**Figure 2** Fabrication process flow of magnetic field controlling device

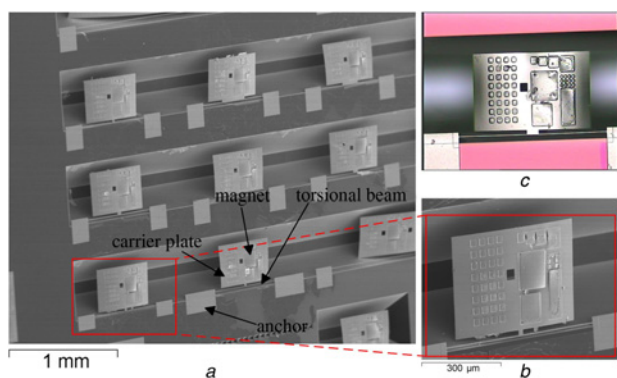
permanent magnetic film of CoNiMnP electrodeposition [21–23], the second layer of Ni was electroplated on the micromagnets' surface to prevent them from the Cu etchant and KOH solution in the subsequent steps. After the seed layer (including Cr and Cu) and the sacrificial layer were removed by their each corresponding etchant, the silicon substrate was deeply etched by KOH solution at  $80^\circ\text{C}$  for about 5 h to release the movable structure.

Compared with the earlier reported microactuators [14–18], we employed KOH wet etching rather than expensive DRIE technology in the bulk micromachining process, which cut down the fabrication cost to a significant degree. KOH etching is a batch process, many wafers can be fabricated at one time. In addition, all the processes in our fabrication process flow are performed on the same wafer side, which means a single side polished wafer can be employed in this fabrication. The sacrificial layer is also important in the process flow, without which the silicon underneath the mirror part will only be etched by an undercut from the edge of the mirror in KOH wet etching process.

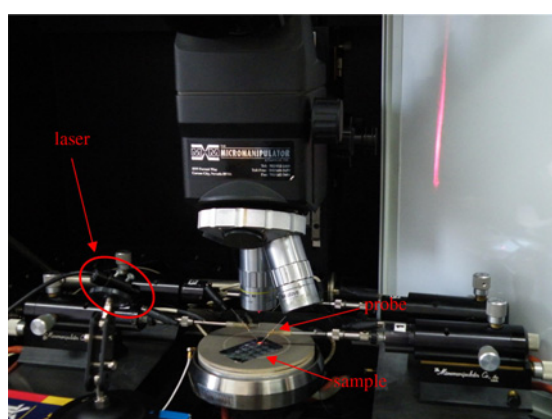
In CoNiMnP permanent magnetic film electrodeposition, external bulk magnets were employed to improve the magnetic properties of the CoNiMnP alloy. To investigate the performance of our electrodeposited micromagnets, we performed magnetic property measurement by an Alternating Gradient Magnetometer, MicroMag 2900 for a magnetic hysteresis loop.

Fig. 3 demonstrates the experimental setup for torsional angle measurement of the microactuator. A spot laser generator, a manual probe station (Micromanipulator Co., Inc.) and a recording white board have been employed. Only two microprobes are needed in this measurement, which are connected to a high-voltage source. The laser focused on the mirror part of the microactuator will be reflected on the recording white board, and the shifting distance of the reflected spot can be converted into the torsional angle of the microactuator.

**4. Result and discussion:** Scanning electron microscope (SEM) pictures of our fabricated modulator array and single device (zoom in view) are shown in Fig. 4. The carrier plate, torsional beam and anchors are formed by Ni electroplating, they play the role of one electrode of the electrostatically driven device,



**Figure 3** Experimental setup  
*a* SEM of microdevices array  
*b* Zoom in view of single device  
*c* Microscope picture of microdevice



**Figure 4** Schematic diagram of driving circuit

whereas another electrode is the silicon substrate, insulated by the  $\text{Si}_3\text{N}_4$  layer underneath the Ni anchors. While performing torsional angle measurement, a DC bias was set between the silicon substrate and the Ni anchors (connected to the carrier plate part through the torsional beam), the carrier plate will perform an out-of-plane motion towards the tilted silicon sidewall, which is formed by anisotropic KOH etching. The torsional microactuator can be operated both in analogue and digital mode. In analogue mode, the torsional plate can rotate over a continuous angle from  $0^\circ$  to  $18^\circ$ . In digital mode, the torsional plate will be attached to or released from the tilted silicon sidewall by the pull-in effect, a full swing torsional angle of  $54.7^\circ$  can be achieved. The micromagnets on the carrier plate will perform the same motion with the microactuator both in analogue mode and digital mode, and then the surrounding magnetic field will be changed both in amplitude and direction.

Fig. 5 shows the hysteresis loop of a  $5\text{-}\mu\text{m}$ -thick CoNiMnP magnet array on the torsional plate. With the measured remanence and coercivity of magnetic films, the distribution of the generated magnetic field was simulated in the surrounding space. Theoretical data from the analytical model mentioned above has been compared with torsional angle measurement, and it can be seen from Fig. 6*a* that the experimental data fit well with the theoretical data from  $0^\circ$  to  $10^\circ$  of torsional angle. When the torsional angle exceeds  $10^\circ$ , the reflected laser spot comes out of the recording range of our experimental setup, thus no measurement data have been obtained in this range. In fact, the continuous torsional angle can reach  $18^\circ$  according to theoretical simulation and approximate observation in the microscope. The pull-in voltage has been

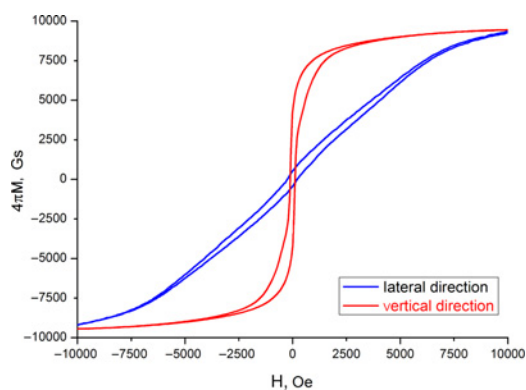


**Figure 5** Hysteresis loop of CoNiMnP magnet film sample

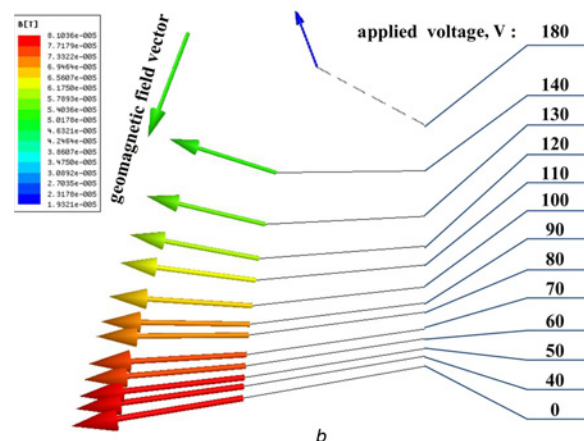
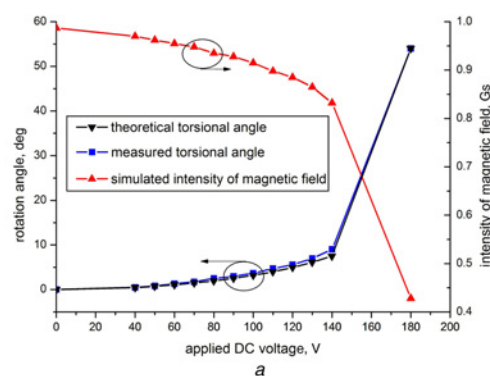


**Figure 6** Modulation of magnetic field  
*a* Intensity modulation and torsional angle of micromodulator  
*b* Direction modulation with respect to driving voltage (colour of arrows indicates the amplitude of magnetic field)

measured to be an average value of  $180\text{ V}$ , while the pull-in angle is  $54.7^\circ$ . With the combination of the measured torsional angle with respect to the applied voltage, the modulation of the magnetic field at a particular position ( $100\text{ }\mu\text{m}$  above micromagnets) has been determined both in intensity and vector direction, as shown in Figs. 6*a* and *b*, respectively.

Compared with the magnitude of the geomagnetic field ( $0.4\text{--}0.6\text{ Gs}$  in magnitude in the overwhelming majority of zones on earth), our generated magnetic field is strong enough to be a modulating source and to be sensed by the magneto-receptors of migratory birds at a certain distance. Nevertheless, while considering the details of biological implantation and other problems in remote navigation, the magnetic modulating performance of the present device still needs to be enhanced. For example, the generated magnetic field can be strengthened by enlarging and thickening the micromagnets

which thus can stimulate the magneto-receptors of migratory birds from a farther implanting position, however the increasing volume of micromagnets will also cause crack and performance degeneration of micromagnets because of increasing residual stress. Hence, how to increase the volume of micromagnets and controlling the residual stress in electroplating is what we shall try in further investigation.

On the other hand, our magnetic field modulator has its own advantage over traditional devices like block magnets [8] and Helmholtz coils [9, 10] formerly employed by avian behaviour researchers in magnetic navigation. Many studies in the behaviour of migratory birds [6–8] have indicated that the direction of the geomagnetic field which provides compass information seems to be playing a more important role in avian navigation, which means that migratory birds maybe not so sensitive to the pure change of intensity of the magnetic field. As a result, novel remotely controlled systems which can precisely modulate the direction of the magnetic field will perform more effective and sensitive navigation for migratory birds than traditional pure magnetic field intensity modulation systems. Our novel magnetic field modulator can be operated in analogue mode and rotates over a continuous angle from 0° to 18°, which cannot be completed by traditional block magnets and Helmholtz coils. Besides, taking advantage of the low working consumption of our novel modulator, the weight of batteries, which takes a large portion in the weight of the whole system, can be significantly reduced. Since the homing pigeon cannot load too heavy controlling systems (no more than 200 g, which differs from pigeon's weight, training experience and flying distance), low power consumption system will be a good choice. In addition, low-power consumption will also achieve a longer working lifetime of the controlling system and less thermal dissipation problems. In a word, our low-power consumption magnetic field micromodulator, which can rotate over a continuous angle from 0° to 18° and effectively modulate the direction of the magnetic field, will be the critical component in the next generation of remotely controlled avian navigation systems.

Furthermore, the electrostatically driven plate of our micromodulator is not only a carrier of hard magnetic films, it can also be integrated with meta material [22, 23] or any other functional material which can be deposited by electroplating. If there is any compatibility problem in the fabrication process flow, another passivation layer can be electroplated in succession to prevent functional material from KOH solution or seed layer etchant.

**5. Conclusion:** We have presented the working principle, analytical model, fabrication process flow and performance measurement of a novel magnetic field modulator. The low power consumption microdevice can modulate the surrounding magnetic field with a continuous modulating angle from 0° to 18° and large shifting range of 54.7°, which is suitable for application of avian magnetic navigation. Unlike the traditional magnetic field exciting components, the present micromodulator can continuously modulate the direction of the magnetic field in a very large shifting range, which has been proved to be a more effective and sensitive device for avian magnetic navigation. In addition, we are not only providing a microactuator for magnetic field modulating, but also a torsional microcarrier which can be integrated with some other functional material, or a novel approach to realise the motion of functional material for relevant researchers.

**6. Acknowledgment:** The authors thank the staff of the National Key Laboratory of Micro/Nano Fabrication Technology in Peking University for cooperation and help in the fabrications. They also thank S. Liu from the School of Physics, Peking University, for help in magnetic property measurement.

## 7 References

- [1] Cugat O., Delamare J., Reyne G.: 'Magnetic micro-actuators and systems (MAGMAS)', *IEEE Trans. Magn.*, 2003, **39**, (5), pp. 3607–3612
- [2] Gibbs M., Hill E.W., Wright P.J.: 'Magnetic materials for MEMS applications', *J. Phys. D, Appl. Phys.*, 2004, **37**, (22), pp. 237–244
- [3] Gibbs M.: 'Applications of magmems', *J. Magn. Magn. Mater.*, 2005, **290**, pp. 1298–1303
- [4] Niarchos D.: 'Magnetic MEMS: key issues and some applications', *Sens. Actuators A*, 2003, **109**, pp. 166–173
- [5] Arnold D.P., Wang N.G.: 'Permanent magnets for MEMS', *J. Microelectromech. Syst.*, 2009, **18**, (6), pp. 1255–1266
- [6] Wiltshcko W., Wiltshcko R.: 'Magnetic orientation and magnetoreception in birds and other animals', *J. Comp. Physiol. A, Neuroethol. Sens. Neural Behav. Physiol.*, 2005, **8**, pp. 675–693
- [7] Mora C.V., Davison M., Wild J.M., Walker M.M.: 'Magnetoreception and its trigeminal mediation in the homing pigeon', *Nature*, 2004, **432**, pp. 508–511
- [8] Wilzck C., Wiltshcko W., Gunturkun O., Buschmann J.U., Wiltshcko R., Prior H.: 'Learning of magnetic compass directions in pigeons', *Anim. Cogn.*, 2010, **13**, pp. 443–451
- [9] Dennis T.E., Rayner M.J., Walker M.M.: 'Evidence that pigeons orient to geomagnetic intensity during homing', *Proc. Royal Soc. B, Biol. Sci.*, 2007, **274**, (1614), pp. 1153–1158
- [10] Keeton W.T.: 'Magnets interfere with pigeon homing', *Proc. Natl. Acad. Sci. USA*, 1971, **68**, (1), pp. 102–106
- [11] Walcott C., Green R.P.: 'Orientation of homing pigeons altered by a change in the direction of an applied magnetic field', *Science*, 1974, **184**, (4133), pp. 180–182
- [12] Visalberghi E., Alleva E.: 'Magnetic influences on pigeon homing', *Biol. Bull.*, 1979, **156**, (2), pp. 246–256
- [13] Liu K., Cao Y.T., Yu H.Q., Li Z.H.: 'A microactuator for magnetic field control device with large shifting range'. Proc. 8th Annual IEEE Int. Conf. on Nano/Micro Engineered and Molecular systems, Suzhou, China, April 2013
- [14] Toshiyoshi H., Fujita H.: 'Electrostatic micro torsion mirrors for an optical switch matrix', *J. Microelectromech. Syst.*, 1996, **5**, pp. 231–237
- [15] Wu W.G., Li D.C., Sun W., Hao Y.L., Yan G.Z., Jin S.J.: 'Fabrication and characterization of torsion-mirror actuators for optical networking applications', *Sens. Actuators A*, 2003, **108**, pp. 175–181
- [16] Tsai J.M.L., Chu H.Y., Hsieh J., Fang W.L.: 'The BELST II process for a silicon high-aspect-ratio micromachining vertical comb actuator and its applications', *J. Micromech. Microeng.*, 2003, **14**, pp. 235–241
- [17] Hah D., Patterson P.R., Nguyen H.D., Toshiyoshi H., Wu M.C.: 'Theory and experiments of angular vertical comb-drive actuators for scanning micromirrors', *IEEE J. Sel. Top. Quantum Electron.*, 2004, **10**, pp. 505–513
- [18] Xie H.K., Pan Y.T., Fedder G.K.: 'A CMOS-MEMS mirror with curled-hinge comb drives', *J. Microelectromech. Syst.*, 2003, **12**, pp. 450–456
- [19] Degani O., Socher E., Lipson A., Leitner T., Setter D.J., Kaldor S., Nemirovsky Y.: 'Pull-in study of an electrostatic torsion microactuator', *J. Microelectromech. Syst.*, 1998, **7**, pp. 373–379
- [20] Zhang X.M., Chau F.S., Quan C., Lam Y.L., Liu A.Q.: 'A study of the static characteristics of a torsional micromirror', *Sens. Actuators A*, 2001, **90**, pp. 73–81
- [21] Liakopoulos T.M., Zhang W.J., Ahn C.H.: 'Electroplated thick CoNiMnP permanent magnet arrays for micromachined magnetic device applications'. IEEE Proc. 9th Annual Int. Workshop on Micro Electro Mechanical Systems, 'An investigation of micro structures, sensors, actuators, machines and systems', San Diego, CA, USA, February 1996
- [22] Watts C.M., Liu X.L., Padilla W.J.: 'Metamaterial electromagnetic wave absorbers', *Adv. Mater.*, 2012, **24**, pp. 98–120
- [23] He X.J., Wang Y., Wang J.M., Gui T.L.: 'MEMS switches controlled multi-split ring resonator as a tunable metamaterial component', *Microsyst. Technol.*, 2010, **16**, pp. 1831–1837
- [24] Shan G., Nelson B.J.: 'Electrodeposition of low residual stress CoNiMnP hard magnetic thin films for magnetic MEMS actuators', *J. Magn. Magn. Mater.*, 2005, **292**, pp. 49–58
- [25] Sun X.M., Yuan Q., Fang D.M., Zhang H.X.: 'Electrodeposition and characterization of CoNiMnP permanent magnet arrays for MEMS sensors and actuators', *Sens. Actuators A*, 2012, **188**, pp. 190–197